Analytical Study on Torsional Behavior of Concrete Beams Strengthened with Fiber Reinforced Polymer Laminates Using Softened Truss Model

Muhanad M. Majed[1], Mohammadreza Tavakkolizadeh[*2], Abbas A. Allawi[3]

1- Graduate Student, Department of Civil Engineering, Ferdowsi University of Mashhad, Iran. E-mail: al-deraan9526411020@mail.um.ac.ir

2- Assistant Professor, Department of Civil Engineering, Ferdowsi University of Mashhad, Iran. E-mail: drt@um.ac.ir

3- Professor, Department of Civil Engineering, University of Baghdad, Iraq. E-mail: a.allawi@uobaghdad.edu.iq

Corresponding author: Mohammadreza Tavakkolizadeh, Assistant Professor, Department of Civil Engineering, Ferdowsi University of Mashhad, Iran.

Email: drt@um.ac.ir

ORCID: 0000000209324605

Tel/Fax: +98 513 8806021

Analytical Study of Torsional Behavior of Concrete Beams Strengthened with Fiber Reinforced Polymer Laminates Using Softened Truss Model

Abstract: This study aimed at evaluating the torsional capacity of reinforced concrete (RC) beams externally wrapped with fiber reinforced polymer (FRP) materials. An analytical model was described and used as a new computational procedure based on the softened truss model (STM) to predict the torsional behaviour of RC beams strengthened with FRP. The proposed analytical model was validated with the existing experimental data for rectangular sections strengthened with FRP materials and considering torque-twist relationship and crack pattern at failure. The confined concrete behavior, in the case of FRP wrapping, was considered in the constitutive laws of concrete in the model. Then, an efficient algorithm was developed in MATLAB environment to accomplish the analysis, solve the appropriate equations, and calculate the torsional moment and angle of twist at all points. The parametric study considered the effect of effective fiber strain to reach a better prediction for the full torsional behavior. The model was able to predict the torsional behaviour of the RC beams strengthened with FRP materials before and after cracking stages with reasonable accuracy.

Keywords: Torsion, Angle of Twist, RC Beams, Softened Truss Model (STM), FRP Strengthening

INTRODUCTION

Reinforced concrete (RC) members in a structure may be subjected to loads with magnitudes greater than those considered as design loads. Axial forces, shear forces, bending moments, torsion, or a combination of these effects are considered to design a safe structural member. Fiber Reinforced Polymer (FRP) laminates have been used to repair and retrofit RC members under axial forces, bending moments, and shear forces in the past two decades. Several researchers have conducted experimental and numerical studies to predict the behaviour of FRP-strengthened members (Keykha, 2020; Saadatmanesh and Ehsani, 1990; Hassan and Rizkalla, 2004; Bae et al., 2013; Karbhari, 2004). Flexural and shear strengthening could cause premature debonding of FRP laminates and has been the subject of different studies in the past (Rasheed et al., 2011; Shukri et al., 2020). In most design situations, these types of loadings are considered as primary effects, whereas torsional moment is regarded as secondary. Therefore, torsional behavior of RC beams is not studied as much in depth as their behavior under different loadings. Torsion could become a primary effect for spandrel or curved beams (Ghobarah et al., 2002).

Panchacharam and Belarbi (2002) experimentally studied the behavior and performance of RC members strengthened with glass fiber-reinforced polymer (GFRP) sheets and considered different numbers of GFRP layers, fiber orientations, arrangements, and configurations. Hii and Al-Mahaidi (2006) recounted an experimental work which investigated the torsional strengthening of solid and box-section reinforced concrete beams with externally bonded carbon fiber reinforced polymer (CFRP) sheets. Allawi (2006) modified and extended the existing softened membrane model (SMM) theory to be applicable to nonlinear torsional analysis of RC members. Ameli and Ronagh (2007) presented the results of experimental and numerical study of RC beams strengthened with FRP sheets under pure torsion in a variety of configuration.

Another study by Deifalla and Ghobarah (2010) resulted in proposing an analytical model capable of predicting the full torsional behavior of RC beams wrapped with FRP sheets up to failure. The model took into account several possible strengthening techniques including continuous wrapping, spiral wrapping, one-sided wrapping, and strips wrapping. Zojaji and Kabir (2012) developed a new computational procedure to obtain the full torsional behavior of RC beams strengthened with FRP based on the SMM for torsion.

Previous researchers developed some equations based on the softened truss model (STM) for torsion problem (Hsu, 1988; Hsu, 1990; Hsu, 1991; Hsu, 1992; HSU, 1993; Collins and Mitchell, 1991; Hareendran et al., 2019). Chalioris (2007) proposed an analytical model based on the STM theory in combination with two other different theoretical models including the smeared crack model and the modified softened truss model theory. To predict the entire behavior of the strengthened beams under torsion, Chai et al. (2015) proposed a new analytical method for predicting the torsional capacity and behavior of RC multicellular box girders strengthened with CFRP sheets. Ramancha et al. (2015) improved the proposed model based on the STM to predict the response of RC members under torsional loading. Shen et al. (2018) proposed a model that additionally addresses the effect of concrete on tension based on the previous modified STM for torsion.

In the present study, the aim was torsional strengthening of RC beams using externally bonded FRP materials, which is a recent development and remains an open field of research. Another objective was to extend and modify the existing STM algorithm to enable a nonlinear torsional analysis that takes into consideration the effect of the confinement developed by CFRP sheet in concrete. The developed model was validated by the experimental data obtained from different studies. Analytical and experimental results that included full torque-twist curves of FRP-strengthened RC beams (continuous sheets and strips) in various retrofitting configurations were also compared and extensively discussed. The parametric study considered the effect of effective fiber strain to reach a better prediction for the full torsional behavior. The findings of this study may provide useful information for future studies in this field.

ANALYTICAL MODEL

After concrete beams cracking, torsion is resisted by the truss action of compressive stresses in diagonal concrete struts, tensile stresses in longitudinal bars, transverse stirrups, and FRP external reinforcement. For calculating the post-cracking torsional behavior of FRP-strengthened RC beams, the analytical model is used based on the STM, which is based on the analytical procedures presented by Chalioris (2007) and Chai et al. (2015). The model was first mentioned by Hsu and Mo (1985) and was well known for torsion, and later it was adopted and modified to include the FRP strengthening effect.

In the present study, equilibrium and compatibility equations were solved in conjunction with the constitutive laws of an element taken from a member subjected to pure torsion; this approach is extended to include the influence of FRP strengthening on torsional response. Moreover, the confinement of concrete as a result of FRP wrapping through the beam section was considered in constitutive laws of concrete. A trial and error algorithm in MATLAB environment was developed to calculate each point of the torque-twist curve.

Equilibrium Equations

Fig. 1(a) presents an FRP-strengthened RC prismatic member subjected to an external torque (T). This torque is resisted by an internal torque formed by the circulatory shear flow (q) along the periphery of the cross section, which occupies a shear flow zone of a thickness (t_d). After the concrete member cracking, torsion is resisted by the truss action of the compressive stresses in diagonal concrete struts, tensile stresses in longitudinal bars, transverse stirrups, and FRP external reinforcement (Hsu, 1990).

The applied stresses to the element have three components, namely σ_l; σ_t and τ_{lt}. Longitudinal and transverse steels are arranged in horizontal and vertical axes (l and t axes) with uniform spacing. In this study, the effect of FRP forces was included in the equilibrium equations by considering CFRP sheets as additional external reinforcements. After cracking, the concrete was separated by diagonal cracks into a series of concrete struts, as shown in Fig. 1(b). The cracks were oriented at an angle α with respect to the longitudinal axis. The principal stresses on the concrete strut itself are denoted by σ_d and σ_r.

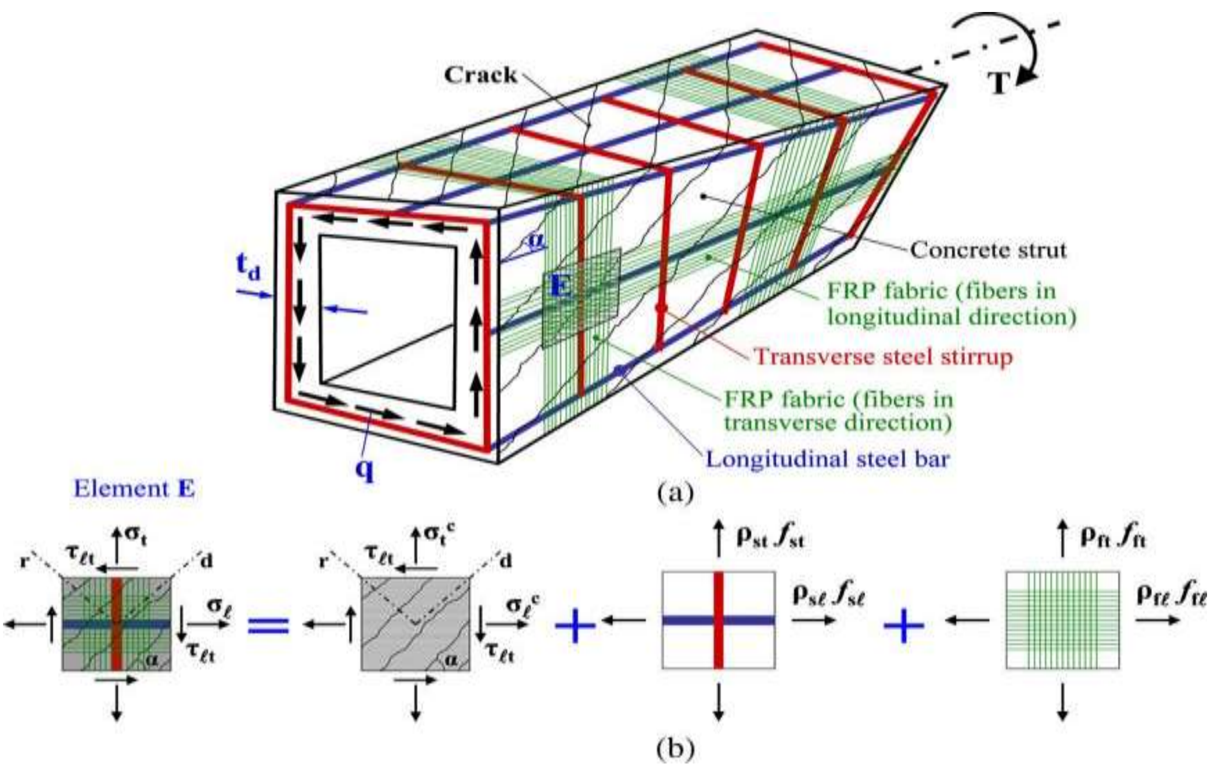

Figure 1: Space truss for the torsional analysis of the reinforced concrete beams strengthened with fiber-reinforced polymer composites (Chalioris, 2007).

According to the unified theory, after transformation, the governing equations for equilibrium condition are as follows (Hsu, 1994):

$$\sigma_l = \sigma_d \, cos^2\alpha + \sigma_r \, sin^2\alpha + \rho_{sl} f_{sl} + \rho_{fl} \, f_{fl} \tag{1}$$

$$\sigma_t = \sigma_d \, sin^2\alpha + \sigma_r \, cos^2\alpha + \rho_{st} f_{st} + \rho_{ft} f_{ft} \tag{2}$$

$$\tau_{lt} = (-\sigma_d + \sigma_r) \, sin \, \alpha \, cos \, \alpha \tag{3}$$

$$T = \tau_{lt}(2A_o t_d) \tag{4}$$

and

$$\tau_{lt} = (-\sigma_d) \, sin \, \alpha \, cos \, \alpha \tag{5}$$

where σ_l, σ_t, and τ_{lt} are the three stress components of the composite element as shown in Figure 1(a) and include normal stresses in the longitudinal and transverse directions and the applied shear stress in $l - t$ coordinates, respectively. σ_d and σ_r are the diagonal principal compressive and diagonal principal tensile stresses in the $d - r$ directions, respectively. α (crack angle) is the angle between the $d - r$ axes; f_{sl}, f_{st}, f_{fl} and f_{ft} are the stresses in steel and FRP in the $l - t$ directions, respectively. ρ_{sl}, ρ_{st}, ρ_{fl} and ρ_{ft} ratios are the ratios of steel and FRP in the *l* and *t* directions, respectively. *T* is the external torque, and A_o is the cross-sectional area bounded by the centreline of the shear flow zone. In addition, t_d is the shear flow zone thickness.

The reinforcement and FRP ratios used in the above equations can be calculated by the following expressions:

$$\rho_{sl} = \frac{A_{sl}}{p_o t_d} \tag{6}$$

$$\rho_{st} = \frac{A_{st} p_{st}}{p_0 t_d s} \tag{7}$$

$$\rho_{fl} = \frac{A_{fl}}{p_0 t_d} \tag{8}$$

and

$$\rho_{ft} = \frac{A_{ft} p_{ft}}{p_0 t_d s_f} \tag{9}$$

where $\boldsymbol{A_{sl}}$ and $\boldsymbol{A_{fl}}$ are the total cross-sectional areas of the longitudinal mild steel and longitudinal FRP laminates, respectively. Also, $\boldsymbol{A_{st}}$ and $\boldsymbol{A_{ft}}$ denote the total cross-sectional areas of the transverse mild steel bar and the transverse FRP laminate, respectively. p_0 is the perimeter of the centre line of shear flow zone, $\mathrm{t_d}$ is the width of the shear flow zone, p_{st} is the perimeter of the steel stirrup, p_{ft} is the perimeter of the strengthened RC member cross section in the transverse direction, and s is the stirrup spacing.

Compatibility Equations

Similarly, the plane compatibility of the shear element in Figure 1 should satisfy the following three equations based on the unified theory as follows:

$$\varepsilon_l = \varepsilon_d\, cos^2\alpha + \varepsilon_r\, sin^2\alpha \tag{10}$$

$$\varepsilon_t = \varepsilon_d\, sin^2\alpha + \varepsilon_r\, cos^2\alpha \tag{11}$$

and

$$\frac{\gamma_{lt}}{2} = (-\varepsilon_d + \varepsilon_r)\, sin\,\alpha\, cos\,\alpha \tag{12}$$

where $\varepsilon_l, \varepsilon_t$ and γ_{lt} are the average strains of the steel bars and stirrups in the $l - t$ coordinate. ε_d and ε_r are the average strains in the $d - r$ directions, respectively.

The other compatibility equations relate to the angle of twist per unit length and bending curvature of concrete to shear distortion in the wall as suggested by Jeng and Hsu (2009), as follows:

$$\theta = \frac{P_o}{2\,A_o}\gamma_{lt} \tag{13}$$

$$\psi = \theta\, sin\, 2\alpha = \frac{P_0}{2A_0}\gamma_{lt}\, sin\, 2\alpha \tag{14}$$

and

$$\varepsilon_d = \frac{-\varepsilon_{ds}}{2} \tag{15}$$

where θ denotes the angle of twist of a member, P_o is the perimeter of the centreline of shear flow zone, ψ is the bending curvature of the concrete struts, and ε_{ds} is the maximum strain of the concrete struts.

Constitutive Relationships of Materials

The stress–strain relationship used in the proposed model is the one developed by Belarbi and Hsu (1995) for a softened compressive concrete, which was later modified by Chalioris (2007) to include the effect of FRP confinement by using the parameters proposed by Vintzileou and Panagiotidou (2008) as follows:

$$\sigma_d = \sigma_p \left[2\frac{\varepsilon_d}{\varepsilon_p} - \left(\frac{\varepsilon_d}{\varepsilon_p}\right)^2\right] \quad For\ \frac{\varepsilon_d}{\varepsilon_p} \leq \quad 1 \qquad (16)$$

$$\sigma_d = \sigma_p \frac{\varepsilon_d}{\varepsilon_p} \qquad For \qquad \frac{\varepsilon_d}{\varepsilon_p} > \quad 1 \qquad (17)$$

$$\sigma_p = k\ \xi f_c' \qquad (18)$$

and

$$\varepsilon_p = k^2\xi\ \varepsilon_o \qquad (19)$$

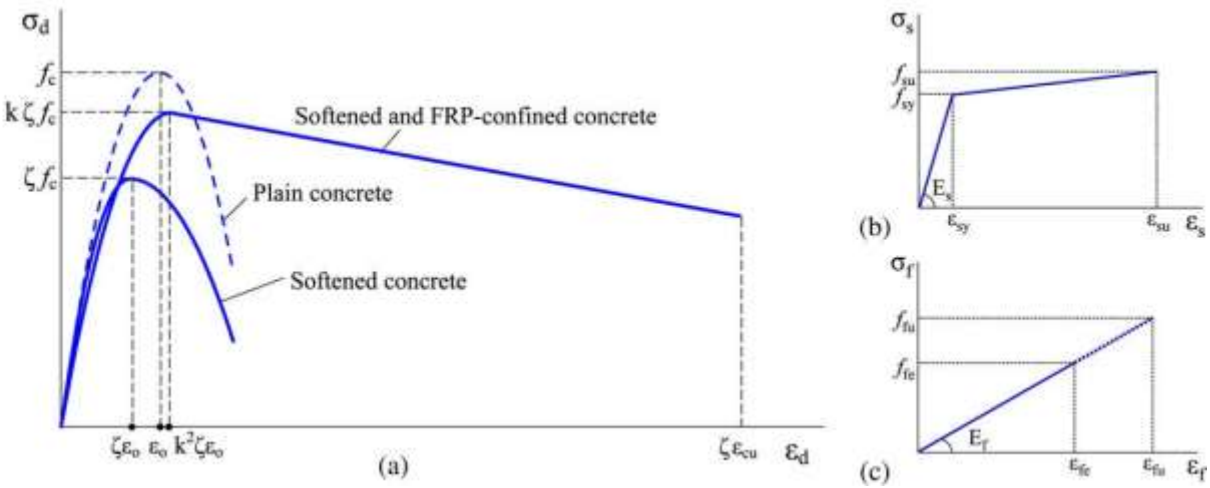

Figure 2: Constitutive stress–strain laws for the materials (Chalioris, 2007)

where f_c' is the concrete cylinder compressive strength, ε_o is the concrete strain at the peak compressive stress taken as −0.002, ζ is the softening coefficient calculated by Eq.

20, and k is the CFRP confinement parameter, which is obtained from a simple empirical equation expressed as Eq. 21:

$$\zeta = \frac{0.9}{\sqrt{1+400\,\varepsilon_r}} \tag{20}$$

and

$$k = 1 + 2.8\,\alpha_n w_w \tag{21}$$

The confinement parameter k of the empirical model for the FRP-confined concrete, which was proposed by Vintzileou and Panagiotidou (2008) was considered:

$$\alpha_n = 1 - \frac{b^2+h^2}{3\,A_c} \tag{22}$$

where α_n is the in-section coefficient confinement calculated by the cross-section dimensions b and h. The parameter ω_w denotes the volumetric mechanical ratio for the external FRP-confinement, expressed as:

$$\omega_w = \frac{Volume\ of\ FRP\ material}{Volume\ of\ the\ confined\ concrete\ core}\,\frac{f_{fu}}{f_c'} \tag{23}$$

where f_{fu} is the ultimate tensile strength of the FRP.

The stress–strain relationship for steel bars, which is used in STMT, is as follows:

$$f_s = E_s\varepsilon_s \qquad for\ \ \varepsilon_s \le \varepsilon_n \tag{24a}$$

$$f_s = f_y\left[(0.9-2B) + (0.02+0.25B)\frac{\varepsilon_s}{\varepsilon_y}\right] \qquad for\ \ \varepsilon_s > \varepsilon_n \tag{24b}$$

where

$$B = \left(\frac{f_{cr}}{f_y}\right)^{1.5} \Big/ \rho \tag{25}$$

$$\varepsilon_n = \varepsilon_y(0.93-2B) \tag{26}$$

The stress–strain relationships for the FRP and the effective strain in the principal material direction (ε_{fe}) are estimated using the following analytical approaches. The model of

Triantafillou and Antonopoulos (2000), which has been adopted in fib Bulletin 14 (2001), is considered as:

$$\varepsilon_{fe} = 0.17 \left(\frac{f_c^{\frac{2}{3}}}{E_f\, \rho_f} \right)^{0.30} \varepsilon_{fu} \tag{27}$$

For U-jacketing and rupture or peeling-off failure:

$$\varepsilon_{fe} = min \begin{cases} 0.17 \left(\frac{f_c^{2/3}}{E_f \rho_f} \right)^{0.3} \varepsilon_{fu} \\ 0.65 \left(\frac{f_c^{2/3}}{E_f \rho_f} \right)^{0.65} \times 10^{-3} \end{cases} \tag{28}$$

The equation was rearranged to calculate the effective strain in the CFRP composite laminate as proposed by Ghobarah et al. (2002) and Salom et al. (2004).

A value of 0.004 for the characteristic effective CFRP strain suggested in ACI440.2R-17 (2017) is shown to be the optimum value for design purposes, and it was used in this study to reach a better prediction for the full torsional behavior.

$$\varepsilon_{fe} = \frac{T_f\, S}{2A_0 A_f E_f (\cos\alpha + \sin\alpha)} \tag{29}$$

The effective stress of FRP is calculated by Hooke's law using the modulus of elasticity of the FRP (E_f).

$$f_{fe} = \varepsilon_{fe}\ E_f \tag{30}$$

The thickness of shear flow zone (t_d) can be expressed in terms of strains using the compatibility equations and in terms of A_o and P_o as shown below:

$$t_d = \frac{A_o}{P_o} \left[\frac{(-\varepsilon_d)(\varepsilon_r - \varepsilon_d)}{(\varepsilon_l - \varepsilon_d)(\varepsilon_t - \varepsilon_d)} \right] \tag{31}$$

The strain ε_l can be related to the stress f_l by eliminating the angle α from the equilibrium equation.

$$\varepsilon_l = \varepsilon_d + \frac{A_o(\varepsilon_d)(-\sigma_d)}{A_l f_l + A_{lf} f_{lf}} \tag{32}$$

Similarly, the strain ε_t can be related to the stress f_t by eliminating the angle α from the equilibrium equation.

$$\varepsilon_t = \varepsilon_d + \frac{A_o\, s(\varepsilon_d)(-\sigma_d)}{P_o\left(A_t f_t + A_{tf} f_{tf}\right)} \tag{33}$$

Also, A_o and P_o can be expressed as functions of t_d:

$$A_o = A_c - \frac{1}{2} P_c\, t_d + t_d^2 \tag{34}$$

$$P_o = P_c - 4t_d \tag{35}$$

where the cross-sectional area (A_c) is bounded by the outer perimeter of the concrete ($P_{c)}$.

The values of ε_r and $\propto$ can be expressed in terms of strains ε_l, ε_t and ε_d by:

$$\varepsilon_r = \varepsilon_l + \varepsilon_t - \varepsilon_d \tag{36}$$

and

$$tan^2\alpha = \frac{\varepsilon_l - \varepsilon_d}{\varepsilon_t - \varepsilon_d} \tag{37}$$

The solution algorithm steps illustrated in the flowchart shown in Figure 3 were applied using MATLAB by running the trial and error procedure to calculate each point of the torsional moment-twist per unit length. In this study, the contribution of the composite fibers in the transverse (wrap) direction $\left(\rho_{ft} f_{ft}\right)$ was considered. In fact, ε_d varies monotonically from zero to maximum. The maximum values of the main variables in this study (ε_d) spanned from 0.00035 to 0.001.

After inputting the geometry parameters and the material properties of the beam, the ε_d, ε_r and t_d values were selected, and iterative loops were executed until ε_d or ε_f reached its maximum value. Then, all the unknown variables were out putted and the curves related to all the variables were plotted, especially the $T - \theta$ curve.

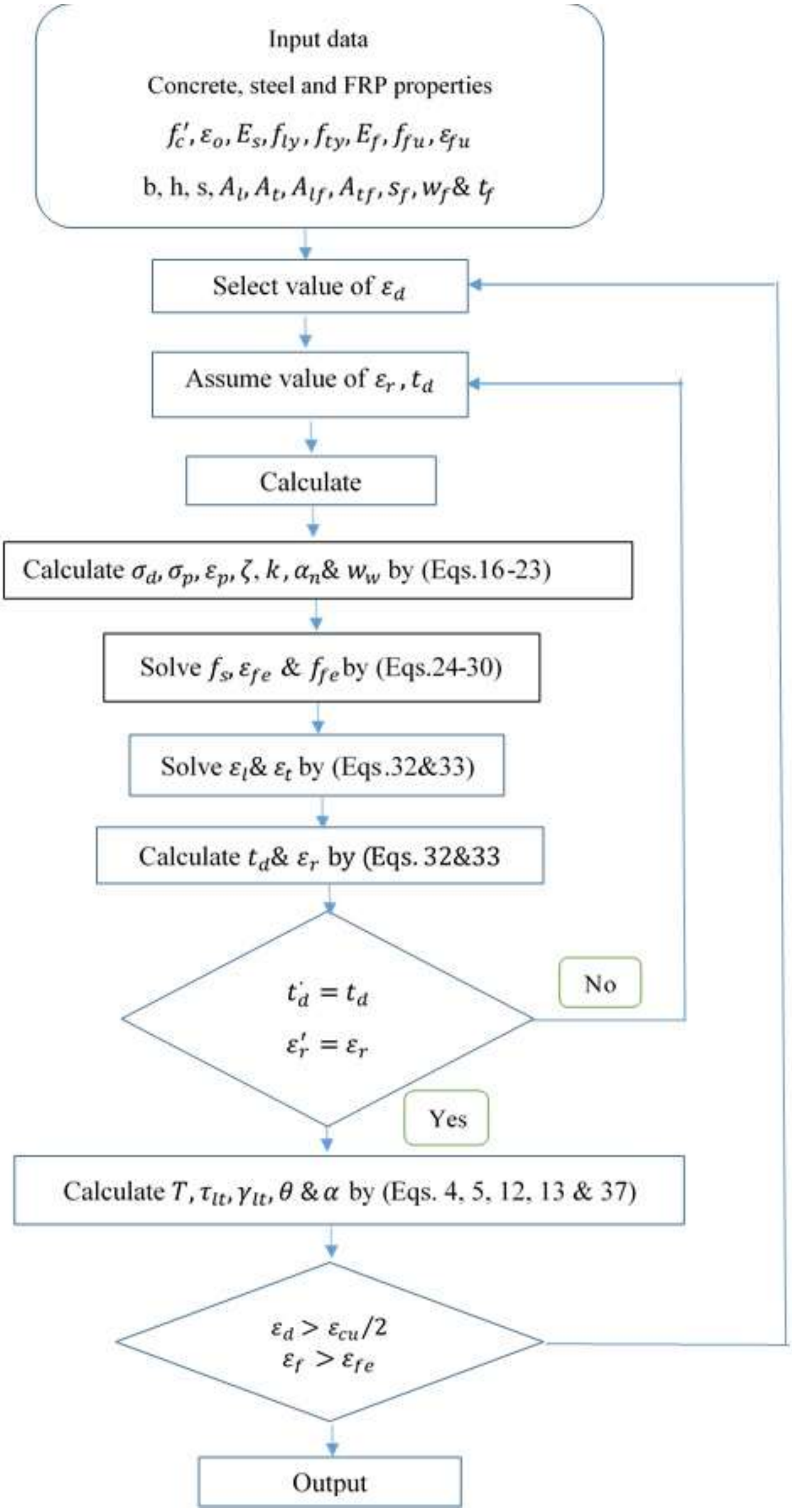

Figure 3: Unified solution algorithm for solid RC members

MODEL VALIDATION

The model was validated by comparing the predicted response with the responses obtained experimentally for different specimen tested by several researchers (Ghobarah et al., 2002; Panchacharam and Belarbi, 2002; Allawi, 2006; Ameli and Ronagh, 2007; Hii and Al-Mahaidi, 2006; Alabdulhady and Sneed, 2018; Majeed et al., 2017; Mirzaei Hesari and Tavakkolizadeh, 2018). The cracking, ultimate torque, and twist values obtained from the analytical and experimental results were generated based on the STM for unstrengthened RC beams as presented by Hsu and Mo (1985). Then, modifications based on Chalioris (2007) as discussed in the Analytical Model section were implemented to predict the $T - \theta$ response for the strengthened beams. The analytical results are summarized and compared with the experimental results in "Torsional Moment– Twist per unit length". The experimental data of 45 solid beams strengthened with FRP materials obtained from the literature was collected. The geometry parameters and the material properties of the collected beams are shown in Table 1. All the test beams had rectangular cross sections with longitudinal steel bars, stirrups, and external FRP materials. The wrapping schemes of the FRP materials for the beams were fully wrapped with continuous sheets or strips.

TORSIONAL RESPONSE

Theoretical analysis using the analytical model was performed to predict the entire torsional behavior of the RC beams strengthened with FRP materials. The sample

Table 1. Physical properties of the concrete beams strengthened with fiber-reinforced polymer

Beam	b/h (mm/mm)	f_c' (MPa)	A_l (mm^2)	f_{ysl} (MPa)	A_t/s (mm)	f_{yst} (MPa)	FRP configuration
Chalioris study (2008)							
Ra-F(1)	100/200	27.5	201	560	-	-	Full wrapping with sheets
Ra-F(2)	100/200	27.5	201	560	-	-	Full wrapping with sheets
Ra-Fs150(2)	100/200	27.5	201	560	-	-	Wrapping with strips
Rb-F(1)	150/300	28.8	201	560	-	-	Full wrapping with sheets

Rb-Fs200(1)	150/300	28.8	201	560	-	-	Wrapping with strips
Rb-Fs300(1)	150/300	28.8	201	560	-	-	Wrapping with strips
Panchacharam and Belarbi study (2002)							
A90w4	279/279	34	792	420&460	0.468	420	90 degree complete wrap
A90S4	279/279	34	792	420&460	0.468	420	90 degree strips
C90U3	279/279	31	792	450&320	0.468	420	90 degree U-wrap
B9U3	279/279	26	792	450&320	0.468	420	90 degree U-wrap with anchors
A0L4	279/279	34	792	420&460	0.468	420	0 degree, 4 sides
A0L3	279/279	34	792	420&460	0.468	420	0 degree, 3sides
B0L4/90S4	279/279	26	792	450&320	0.468	420	0 degree, 4 side and 90 degree strips
Hii and Al-Mahaidi study (2006)							
FS050D2	500/350	56.4	1100	398	0.226	426	Full strips (solid)
Ghobarah et al. study (2002)							
C1	150/350	37	603	409&406	0.452	457	All beams wrapped
C2	150/350	37	603	409&406	0.452	457	5 vertical strips of 100 mm spaced 100 mm
C4	150/350	37	603	409&406	0.452	457	3 vertical strips of 200 mm spaced 100 mm
C5	150/350	37	603	409&406	0.452	457	4 vertical strips of 100 mm spaced 150 mm
G1	150/350	37	603	409&406	0.452	457	All beam wrapped
G2	150/350	37	603	409&406	0.452	457	5 vertical strips of 100 mm spaced 100 mm
Ameli and Ronagh study (2007)							
CFE	150/350	39	804	502	0.353	251	All beam wrapped one layer
CFE2	150/350	39	804	502	0.353	251	All beam wrapped two layer
CJE	150/350	39	804	502	0.353	251	All beam wrapped (U-wrapped)
CFS	150/350	39	804	502	0.353	251	Full strips
CJS	150/350	39	804	502	0.353	251	Strips (U-jacket)
GFE	150/350	39	804	502	0.353	251	All beam wrapped one layer
GFE2	150/350	39	804	502	0.353	251	All beam wrapped two layers
GJE	150/350	39	804	502	0.353	251	All beam wrapped (U-wrapped)
GFS	150/350	39	804	502	0.353	251	Full strips
GJS	150/350	39	804	502	0.353	251	Strips (U-jacket)
Allawi study (2006)							
B2	150/150	30	201.06	467	0.327	708	All beam wrapped
B3	150/150	30	201.06	467	0.327	708	All beam wrapped (U-wrapped)
B4	150/150	30	201.06	467	0.327	708	Full strips
B5	150/150	30	201.06	467	0.327	708	Full strips (U-strips)
B6	150/150	30	201.06	467	0.327	708	Full strips (parallel and longitudinal)
Alabdulhady and Sneed study (2018)							
N-P-3-S-1	203.2/304.8	39.3	796	469	0.698	454	3-side wrapping 90^0 strips
N-P-4-S-1	203.2/304.8	39.3	796	469	0.698	454	4-side wrapping 90^0strips
N-P-4-C-1	203.2/304.8	39.3	796	469	0.698	454	90 degrees complete wrap
N-P-4-C-2	203.2/304.8	39.3	796	469	0.698	454	90 degrees complete wrap
Majeed et al. study (2017)							

ST-S	250/350	45	452	605	0.282	402	Strengthened single cell
ST-D	500/350	43	678	605	0.565	402	Strengthened double cell
ST-T	750/350	43	904	605	0.847	402	Strengthened triple cell
Mirzaei and Tavakkolizadeh study (2018)							
B1	150/ 200	35	314	400	0.334	340	Fully and completely wrapped beams with continuous CFRP sheets
B2	150/ 200	35	314	400	0.334	340	U-wrap beams with CFRP
B3	150/ 200	35	314	400	0.334	340	Wrapping with75 mm width strips spaced 110mmwith CFRP

comparison of the STM model and the results from previous experimental studies is shown in Figure 4. Figure 5 shows the results of the parametric study to calculate the effective strain by fib Bulletin 14 (2001), ACI440.2R-17 (2017), Ghobarah et al. (2002), and Salom et al. (2004) used in the STM to obtain an efficient solution algorithm by MATLAB to accomplish the analysis and solve the appropriate equations for calculating the torsional moment and angle of twist.

The values of cracking torque, peak torque, and their corresponding twist obtained from the STM are compared with the experimental data in Table 2. As expected, the STM provided a good prediction on the elastic torsional stiffness of FRP-strengthened RC beams. The average value of $\frac{T_{cr,Exp}}{T_{cr,cal}}$ for the 45 beams strengthened with different FRPs was 0.99 with a standard deviation of 7.5%. Good agreement was obtained between the ultimate torques obtained from the STM and the values from tests, since the mean value and the standard deviation of $\frac{T_{u,Exp}}{T_{u,cal}}$ were 0.97 and 6%, respectively. Based on the above

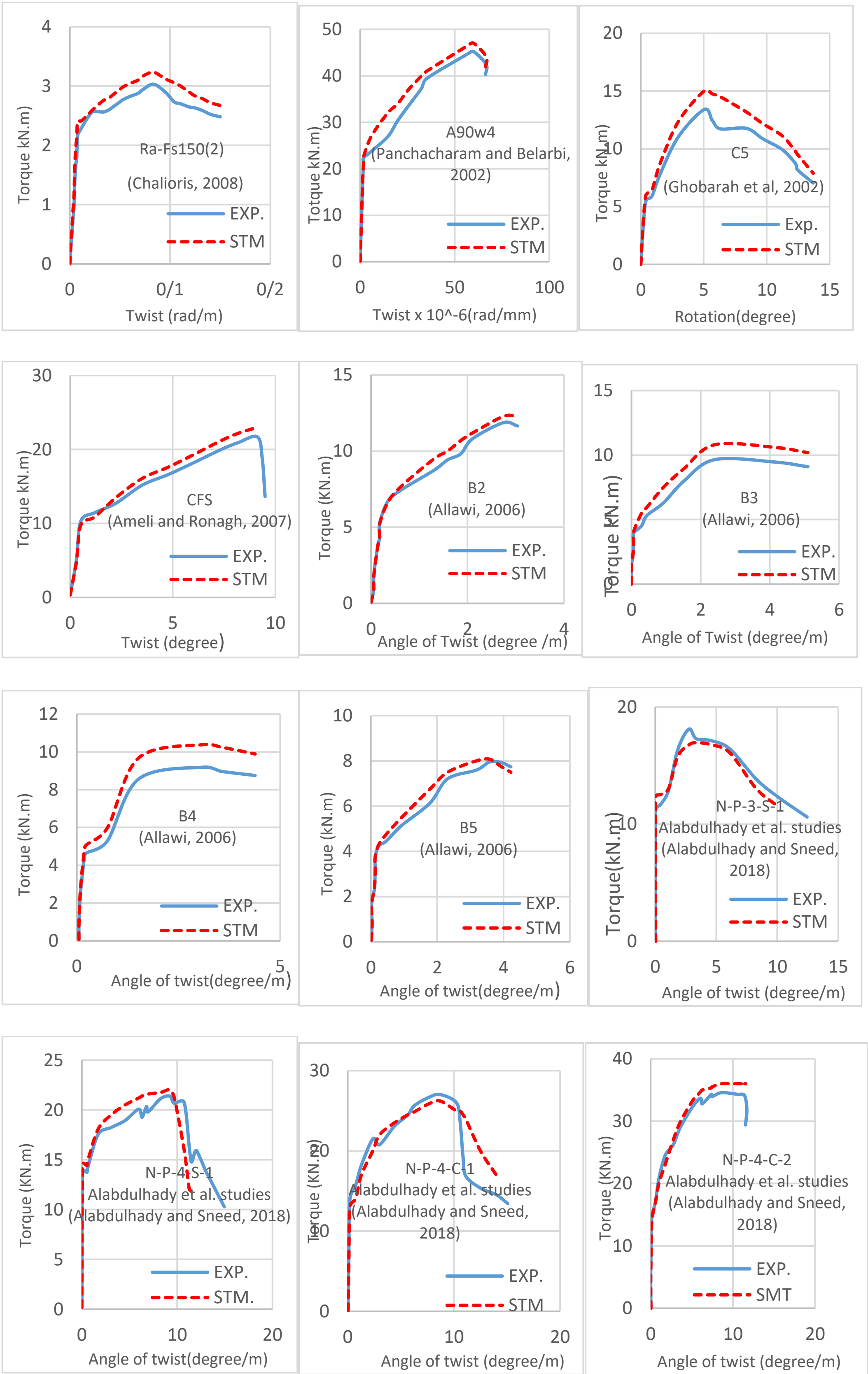

Figure 4 Comparison between output of the STM with experimental curves for beams.

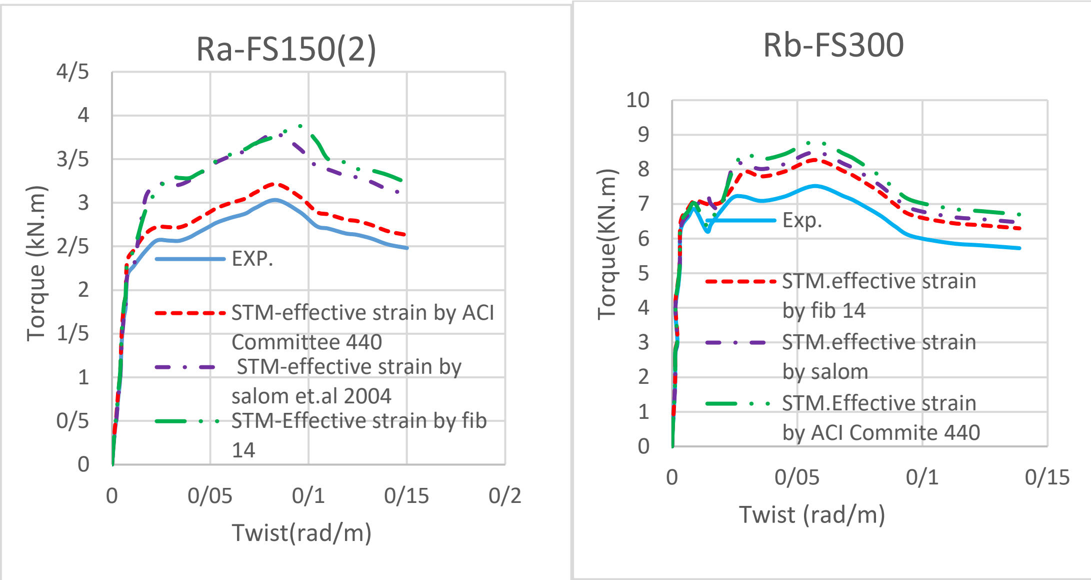

Figure 5: Experimental behavior and comparisons with analytically predicted curves for the FRP strengthened beam tested by chalioris (2008).

analysis, the proposed analytical model of the STM provides a reliable method for the analysis of the overall torsional behaviors of the FRP-strengthened RC beams.

Table 2. Ultimate torque and corresponding twist angle obtained from experiments and calculated from STM

Beam	$T_{cr;Exp}$	$T_{cr;c}$	$\frac{T_{cr;Exp}}{T_{cr;cal}}$	$T_{u;Exp}$	$T_{u;c}$	$\frac{T_{u;Exp}}{T_{u;cal}}$
Chalioris study (2008)						
Ra-F(1)	2.80	2.30	1.21	4.86	5.20	0.93
Ra-F(2)	2.83	2.30	1.22	6.65	5.76	1.15
Ra-Fs150(2)	2.21	2.41	0.92	3.01	3.12	0.96
Rb-F(1)	8.79	8.28	1.06	10.05	10.98	0.91
Rb-Fs200(1)	6.72	7.37	0.91	9.31	10.33	0.90
Rb-Fs300(1)	6.96	7.22	0.96	7.52	8.44	0.89
Mean value			1.04			0.95
Standard deviation			14%			9.97%
Panchacharam and Belarbi study (2002)						
A90w4	22	22.18	0.99	45	46.66	0.96
A90S4	21	22.18	0.94	34	35.76	0.95
C90U3	20	23.02	0.86	24	27.05	0.88
B9U3	21	19.63	1.06	25	24.97	1.00
A0L4	26	26.45	0.98	29	29.47	0.98
A0L3	25	25.39	0.98	26	27.64	0.94
B0L4/90S4	22	22.48	0.97	35	36.19	0.96
Mean value			0.96			0.95

Standard deviation			6%			4%
Hii and Al-Mahaidi study (2006)						
FS050D2	73.70	72.83	0.99	93.80	93.18	0.98
Ghobarah et al. study (2002)						
C1	6.73	6.418	1.04	17.98	18.62	0.96
C2	5.53	6.418	0.86	13.96	15.39	0.90
C4	6.57	6.418	1.02	15.83	15.41	1.02
C5	5.87	6.418	0.91	13.42	15.10	0.88
G1	7.17	6.418	1.11	18.93	19.01	0.99
G2	6.29	6.418	0.98	13.15	14.47	0.90
Mean value			0.98			0.94
Standard deviation			9%			5.6%
Ameli and Ronagh study (2007)						
CFE	10.40	10.85	0.95	28.00	27.30	1.02
CFE2	10.70	10.85	0.98	36.50	34.88	1.04
CJE	10.60	10.01	1.05	20.00	19.57	1.02
CFS	10.30	10.01	1.02	21.70	22.12	0.98
CJS	10.20	10.01	1.01	17.40	17.98	0.96
GFE	9.70	10.09	0.96	26.30	25.30	1.03
GFE2	10.50	10.09	1.04	31.10	30.38	1.02
GJE	10.20	10.09	1.01	19.50	19.48	1.00
GFS	10.50	10.09	1.04	19.90	19.22	1.03
GJS	9.90	10.09	0.98	16.90	17.32	0.97
Mean value			1.04			1.007
Standard deviation			3.5%			2.8%
Allawi study (2006)						
B2	6.74	6.66	1.01	11.86	12.28	0.96
B3	4.52	4.67	0.96	9.62	10.87	0.88
B4	4.65	5.08	0.91	9.19	10.45	0.87
B5	4.24	4.28	0.99	7.94	8.064	0.98
B6	4.74	4.68	1.01	9.36	8.22	1.13
Mean value			0.97			0.96
Standard deviation			4%			10.5%
Alabdulhady and Sneed studies (2018)						
N-P-3-S-1	11.6	12.16	0.95	18.1	17.89	1.01
N-P-4-S-1	14.3	15.05	0.95	21.8	22.79	0.95
N-P-4-C-1	13.7	13.05	1.04	27.2	26.76	1.01
N-P-4-C-2	14.5	13.95	1.03	35.1	36.51	0.96
Mean value			0.99			0.98
Standard deviation			5%			3%
Majeed et al. study (2017)						
ST-S	12.2	12.02	1.01	21.5	20.65	1.04
ST-D	37.7	39.00	0.96	50.3	49.43	1.01
ST-T	57.5	56.41	1.01	95.3	94.45	1.00
Mean value			0.99			1.01
Standard deviation			3%			2%
Mirzaei Hesari and Tavakkolizadeh study (2018)						
B1	4.00	4.72	0.84	14.16	15.4344	0.91
B2	3.76	4.5496	1.07	5.41	5.7346	0.94
B3	3.8	4.218	0.90	6.66	7.5258	1.11

Mean value			0.93			0.98
Standard deviation			11%			10%
Total mean value			0.99			0.97
Total standard deviation			7.5 %			6%

CONCLUSION

The modified analytical model based on the STM was extended to predict nonlinear torsional behaviors of the FRP-strengthened RC beams. Additionally, the equilibrium equations, compatibility equations, and the constitutive relationships of the materials were introduced to include the effect of FRP laminates. In this study, we also incorporated a solution algorithm to determine the unknown variables. Application of the proposed procedure allows for a realistic modeling of the elastic and post-cracking response of FRP-strengthened concrete beams under torsion. According to the comparison of the test results with the findings related to the proposed concrete beams strengthened with FRP laminates, the following conclusions are drawn:

1. The suggested algorithm for solving the related equations for torsional analysis of the strengthened beams was found suitable for practical applications because it could accurately predict the torsional capacity and angle of twist response, including both the pre- and post-cracking behaviours.
2. More reasonable compressive and tensile constitutive relationships of FRP-strengthened concrete under torsional loading are employed in the proposed model.

3. The comparisons between the theoretical values calculated by the STM and the experimental results of the 45 beams collected from the available literature indicated the good prediction of overall torque-twist behaviours of the FRP-strengthened RC beams before and after cracking. The proposed analytical model could also accurately capture cracking torque and peak torque.
4. The results presented by the parametric study to calculate the effective strain in this paper imply that the proposed model closely predicts the overall torque-twist behaviour of the tested beams strengthened with FRP composites based on ultimate torsional moment proposed by fib Bulletin 14 (2001), ACI440.2R-17 (2017), Ghobarah et al. (2002), and Salom et al. (2004) with errors of 1.11, 1.09, and 1.13, respectively.

ACKNOWLEDGMENTS

This research was supported by the Faculty of Engineering at Ferdowsi University of Mashhad under research grant No. 51420. The authors are grateful for the support of the Civil Engineering Department and appreciate the work done by Mr. Mirzaei and staff of the Structures Laboratory.

APPENDIX

Example: Analysing the torsional behaviour of the beam with rectangular cross sections, as shown in Fig. 6. The beam had only longitudinal reinforcement, four deformed bars of diameter 8 mm (4ϕ8) at the corners of the rectangular cross-section. Steel yield strength was 560 MPa for the deformed longitudinal steel bars. The beam is also strengthened with CFRP strips transversely spaced 300 mm center-to-center; the width of each strip is 150 mm, and the thickness of the strip is 0.11 mm. The ultimate tensile strength of the CFRP is 3900 MPa. The cylinder compressive strength of concrete is 27.5 MPa. The tensile strength of concrete is neglected ($\boldsymbol{\sigma_r = 0}$).

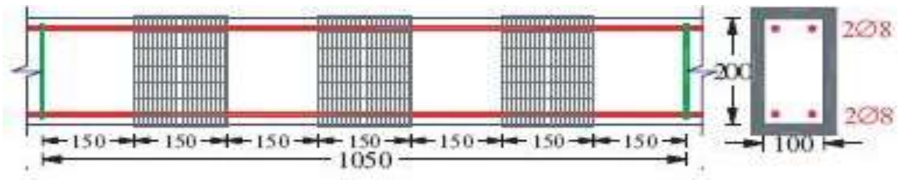

Figure 6: Analysis example of Geometry and reinforcement the tested beam ((Ra-Fs150(2))) by Chalioris study (Chalioris, 2008)

The solution is as follow:

1. Properties of concrete are b=100 mm. h=200 mm. $\varepsilon_o = -0.002$. f_c'= 27.5 MPa. L=1050 mm. E_s=200000. MPa. f_{yl}= 560 MPa. $A_l = 201mm^2$. $\rho_{sl} = 0.01$

2. Properties of CFRP are t_f=0.11mm. w_f=150 mm. s_f=300 mm.$h_f = 200mm$ ε_{fu}=0.015. f_{fu}= 3900 MPa. E_f= 230GPa. ε_{ef}=0.004. $n_f = 2$. $\rho_{fl} = 0.0033$.

3. Assume $\varepsilon_d = -0.0005$

Calculate the area and perimeter of concrete

$A_c = b * h = 20000\ mm^2$

$p_c = 2(b + h) = 600\ mm$

4. Calculate the area and perimeter of fiber

$A_{ft} = n_f w_f t_f$

$A_{ft} = 2 * 150 * 0.11 = 33\ mm^2$

$p_{ft} = 2(w_f + h_f)$=mm

$p_{ft} = 2(150 + 200)$=700 mm

5. The volume of CFRP and confined concrete are

$V_f = p_{ft} t_f w_f n_f$= 0.0033*0.11*150*2 = 0.108

$V_{cc} = A_c w_f n_f$ = 6000000 mm^3

$w_w = V_f \frac{f_{fu}}{V_{cc}(-f_c^{'})}$ = 2.574*10^-6

$\alpha_n = 1 - \frac{b^2+h^2}{3\ A_c}$=0.1667

$k = 1 + 2.8 * \alpha_n w_w$=1.00

$\varepsilon_{cu} = 0.003k\text{^}2 = 0.003$

6. Assume ε_r,t_d

ε_r =0.0022

t_d= 21mm

then

$A_o = A_c - \frac{1}{2} P_c\ t_d + t_d^2$ = 13259mm^2

$P_o = P_c - 4t_d$ =516 mm

$\rho_{ft} = \frac{A_{ft} p_{ft}}{p_0 t_d s_f} = 0.0033$

$\varepsilon_{fe} = 0.17 \left(\frac{f_c^{\frac{2}{3}}}{E_f\ \rho_f} \right)^{0.30} \varepsilon_{fu}$=0.0039

7. Calculate the stress in concrete

$\zeta = \frac{0.9}{\sqrt{1 + 400\ \varepsilon_r}}, \zeta = 0.656$

$\varepsilon_{ds} = \varepsilon_d . 2$, ε_{ds}=-0.001

$\varepsilon_p = k^2 \zeta \, \varepsilon_o$=-0.0013

$\frac{\varepsilon_{ds}}{\varepsilon_p}$ =0.76

$\sigma_p = k \, \xi f'_c = -26.844$

$$\sigma_d = \sigma_p \left[2\frac{\varepsilon_d}{\varepsilon_p} - \left(\frac{\varepsilon_d}{\varepsilon_p}\right)^2 \right] \qquad For \qquad \frac{\varepsilon_d}{\varepsilon_p} \leq \quad 1$$

$$\sigma_d = \sigma_p \frac{\varepsilon_d}{\varepsilon_p} \qquad For \qquad \frac{\varepsilon_d}{\varepsilon_p} > \quad 1$$

$\sigma_d = -11.13 \, MPa$

8. Calculate the strains in the longitudinal and transverse direction, respectively.

$\varepsilon_l = \varepsilon_d + \frac{A_o(\varepsilon_d)(-\sigma_d)}{A_l f_l + A_{lf} f_{lf}}$ = 0.0012

$\varepsilon_t = \varepsilon_d + \frac{A_o \, s(\varepsilon_d)(-\sigma_d)}{P_o(A_t f_t + A_{tf} f_{tf})}$ =5.04*10^-4

$\varepsilon_r = \varepsilon_l + \varepsilon_t - \varepsilon_d$=0.0021

9. Calculate the effective thickness.

$t_d = \frac{A_o}{P_o} \left[\frac{(-\varepsilon_d)(\varepsilon_r - \varepsilon_d)}{(\varepsilon_l - \varepsilon_d)(\varepsilon_t - \varepsilon_d)}\right]$= 20.5 mm

then

α =52^0

τ_{lt}=5.39 MPa

γ_{lt} =0.0026

T =3.12 kN.m

θ = 0.1316 rad/m

REFERENCES

ACI 440.2R-17 (2017) Guide for the design and construction of externaly bonded FRP systems for strengthening concrete structures. American concrete institute, Farmington Hills,MI.

Alabdulhady MY and Sneed LH. (2018) A study of the effect of fiber orientation on the torsional behavior of RC beams strengthened with PBO-FRCM composite. *Construction and Building Materials* 166: 839-854.

Allawi A. (2006) Nonlinear analysis of reinforced concrete beams strengthened by CFRP in torsion. Ph. D. Thesis, University of Baghdad.

Ameli M and Ronagh HR. (2007) Analytical method for evaluating ultimate torque of FRP strengthened reinforced concrete beams. *Journal of Composites for Construction* 11: 384-390.

Bae S-W, Murphy M, Mirmiran A and Belarabi A. (2013) Behavior of RC T-beams strengthened in shear with CFRP under cyclic loading. *Journal of Bridge Engineering* 18: 99-109.

Belarbi A and Hsu TT. (1995) Constitutive laws of softened concrete in biaxial tension compression. *Structural Journal* 92: 562-573.

Chai H, Majeed AA and Allawi AA. (2015) Torsional analysis of multicell concrete box girders strengthened with CFRP using a modified softened truss model. *Journal of Bridge Engineering* 20: B4014001.

Chalioris CE. (2007) Analytical model for the torsional behaviour of reinforced concrete beams retrofitted with FRP materials. *Engineering structures* 29: 3263-3276.

Chalioris CE. (2008) Torsional strengthening of rectangular and flanged beams using carbon fibre-reinforced-polymers–Experimental study. *Construction and Building Materials* 22: 21-29.

Collins M and Mitchell D. (1991) Prestressed Concrete Structures, Prentice Hall, Inc., Englewood Cliffs, N. J.

Deifalla A and Ghobarah A. (2010) Full torsional behavior of RC beams wrapped with FRP: analytical model. *Journal of Composites for Construction* 14: 289-300.

Fib Bulitten 14. (2001) Externally bonded FRP reinforcement for RC structures. *International Federation for Structural Concrete*, CEB-FIP, Lausanne, Switzerland.

Ghobarah A, Ghorbel M and Chidiac S. (2002) Upgrading torsional resistance of reinforced concrete beams using fiber-reinforced polymer. *Journal of Composites for Construction* 6: 257-263.

Hareendran SP, Reddy Kothamuthyala S, Thammishetti N, et al. (2019) Improved softened truss model for reinforced concrete members under combined loading including torsion. *Mechanics of advanced materials and structures* 26: 71-80.

Hassan T and Rizkalla S. (2004) Bond mechanism of NSM FRP bars for flexural strengthening of concrete structures. *ACI Structural Journal* 101: 830-839.

Hii AK and Al-Mahaidi R. (2006) An experimental and numerical investigation on torsional strengthening of solid and box-section RC beams using CFRP laminates. *Composite structures* 75: 213-221.

HSU TC. (1993) Crack angle in unified theory of reinforced concrete. *Studi e ricerche-Politecnico di Milano. Scuola di specializzazione in costruzioni in cemento armato* 14: 279-300.

Hsu TT. (1988) Softened truss model theory for shear and torsion. *Structural Journal* 85: 624-635.

Hsu TT. (1990) Shear flow zone in torsion of reinforced concrete. *Journal of Structural Engineering* 116: 3206-3226.

Hsu TT. (1991) Nonlinear analysis of concrete membrane elements. *Structural Journal* 88: 552-561.

Hsu TT. (1992) Nonlinear analysis of concrete torsional members. *Structural Journal* 88: 674-682.

Hsu TT. (1994) Unified theory of reinforced concrete-A summary. *Structural Engineering and Mechanics* 2: 1-16.

Hsu TT and Mo Y. (1985) Softening of concrete in torsional members-theroy and tests. *Journal Proceedings* 82: 290-303.

Jeng C-H and Hsu TT. (2009) A softened membrane model for torsion in reinforced concrete members. *Engineering structures* 31: 1944-1954.

Karbhari V. (2004) E-glass/vinylester composites in aqueous environments: Effects on short-beam shear strength. *Journal of Composites for Construction* 8: 148-156.

Keykha AH. (2020) Investigation of the behavior of deficient steel members strengthened using carbon fiber reinforced polymer under combined compressive load and torsional moment. *Mechanics of advanced materials and structures* 27: 894-902.

Majeed AA, Allawi AA, Chai KH, et al. (2017) Behavior of CFRP strengthened RC multicell box girders under torsion. *Structural Engineering and Mechanics* 61: 397-406.

Mirzaei Hesari H and Tavakkolizadeh M. (2018) Torsional reinforcement of rectangular reinforced concrete beams using FRP using grooving and reciprocating methods. *Proceedings of the 9th National Concrete Conference of Tehran.* Tehran, Iran.

Panchacharam S and Belarbi A. (2002) Torsional behavior of reinforced concrete beams strengthened with FRP composites. *First FIB Congress, Osaka, Japan.*

Ramancha MK, Mondal TG and Prakash SS. (2015) Softened Truss Model for FRP Strengthened RC Members Under Torsion Including Tension Stiffening Effect. *Advances in Structural Engineering.* Springer, 513-526.

Rasheed HA, Nassajy M, Al Subaie S, et al. (2011) Suppressing delamination failure mode in concrete beams strengthened with short CFRP laminates. *Mechanics of advanced materials and structures* 18: 194-200.

Saadatmanesh H and Ehsani M. (1990) Fiber composite plates can strengthen beams. *Concrete International* 12: 65-71.

Salom PR, Gergely J and Young DT. (2004) Torsional strengthening of spandrel beams with fiber-reinforced polymer laminates. *Journal of Composites for Construction* 8: 157-162.

Shen K, Wan S, Mo YL and Jiang Z. (2018) Theoretical analysis on full torsional behavior of RC beams strengthened with FRP materials. *Composite structures* 183: 347-357.

Shukri AA, Shamsudin MF, Ibrahim Z and Alengaram UJ . (2020) Parametric study for concrete cover separation failure of retrofitted SNSM strengthened RC beams. *Mechanics of advanced materials and structures* 27: 481-492.

Triantafillou T and Antonopoulos CP. (2000) Design of concrete flexural members strengthened in shear with FRP. *Journal of Composites for Construction* 4: 198-205.

Vintzileou E and Panagiotidou E. (2008) An empirical model for predicting the mechanical properties of FRP-confined concrete. *Construction and Building Materials* 22: 841-854.

Zojaji A and Kabir M. (2012) Analytical approach for predicting full torsional behavior of reinforced concrete beams strengthened with FRP materials. *Scientia Iranica* 19: 51-63.